Reviews

Pulse mechanochemistry of organoelement compounds

A. I. Aleksandrov,[a] I. A. Aleksandrov,[a] A. I. Prokof'ev,[b] and N. N. Bubnov[b]*

[a]N. S. Enikolopov Institute of Synthetic Polymer Materials, Russian Academy of Sciences, 70 ul. Profsoyuznaya, 117393 Moscow, Russian Federation. Fax: +7 (095) 420 2229. E-mail: aleks@ispm.ru

[b]A. N. Nesmeyanov Institute of Organoelement Compounds, Russian Academy of Sciences, 28 ul. Vavilova, 117813 Moscow, Russian Federation. Fax: +7 (095) 135 5085. E-mail: tuman@ineos.ac.ru

The results of studies of fast mechanochemical reactions initiated by elastic wave pulses (EWP) of 100 μs duration on polycrystalline mixtures under high pressures (4—25 kbar) are summarized. A possible mechanism of the EWP-initiated processes was proposed.

Key words: pulse, mechanochemistry, radical pairs, *o*-semiquinone metal complexes, ultrafine metal particles, rheological explosion, fast self-propagating chemical processes.

Interest in solid state mechanochemical processes has increased in recent years due to the possibility of developing environmentally safe technologies. Mechanochemistry studies the influence of deformation action on the reactivity of solids.[1] For this purpose, high pressure (HP), shear deformation (SD), their combination,[2,3] and impact waves are used as energy vehicles.[4,5]

A wide scope of phenomena from local warming in a small region to emission of high-energy electrons can be observed in the substance under study.[6]

All methods of mechanochemical action on the substance are characterized by the energetic power (the mechanical energy input to the substance per second) and action dose (the total amount of input mechanical energy) whose values are the following: for grinding the substance in a mortar, 100 W g^{-1} and 10^4 J g^{-1}; for treatment of the substance on a Bridgman anvil, 10^3 W g^{-1} and 10^5 J g^{-1}; under impact waves, 10^{10} W g^{-1} and 10^4 J g^{-1}, respectively.[7]

Some energy consumptions are necessary for any mechanochemical processes. For example, fractionation requires an energy of 0.01 MJ mol^{-1}; dispersion and fine dispersion, 0.1 MJ mol^{-1}; organic synthesis, 1 MJ mol^{-1}; and inorganic synthesis and mechanical fusion require up to 100 MJ mol^{-1}.[6] Powers of the action should also differ, because the threshold level beyond which this reaction can occur should be overcome. For example, synthesis of diamonds[8] from graphite occurs under impact waves (when the power of action is maximum) and is impossible at a lower power.

All available experimental approaches possess two substantial disadvantages. First, actions on the solid state matrix cannot be quantitatively estimated, which prevents one from estimating the yield of the mechanochemical reaction. Second, in the majority of devices used (mortars, mills, Bridgeman anvils, disintegrators, extruders, and others), it is impossible to separate thermal and non-thermal processes (related to deformations

Translated from *Izvestiya Akademii Nauk. Seriya Khimicheskaya*, No. 9, pp. 1621—1635, September, 1999.

1066-5285/99/4809-1599 $22.00

only). As mentioned in review,[1] an exact concept on the primary elementary mechanochemical act is absent, and it is not clear which transformations of the substance occur after the mechanical action when the elastic energy is converted to heat but not instantly and not completely. Therefore, unlike photochemistry and radiation chemistry, for which fast processes involving high-energy intermediates of chemical reactions have been studied in detail, in mechanochemistry chemical processes are considered on the basis of final products that appear upon thermal action.

To study intermediate products of mechanochemical reactions, the mechanical energy should be supplied more rapidly than it is converted to the heat, and the products appearing should rapidly be studied,[2] *i.e.*, in fact, experiments similar to pulse photolysis[9] or radiolysis[10] should be performed.

In this review, we generalized the works[11—22] that used a new experimental approach in which the low-intensity elastic wave pulses (EWP) are combined with thermal and matrix stabilization of intermediates. The experimental data on the generation of organic radicals and radical pairs, organometallic complexes, and ultrafine metal particles produced during decomposition of organometallic compounds are analyzed, and possible mechanisms of solid state chemical processes under pulses of elastic waves are discussed.

To study the EWP action on solid samples, we used the device described previously.[13] A sample was simultaneously subjected to uniaxial compression in a closed volume between two steel wave guides and EWP action. The elastic waves were generated during explosive decomposition under pressure (rheological explosion) of polypropylene, polyethylene, or polystyrene plates. Elastic wave pulses reached the samples thermostatted at 77 or 300 K through a steel wave guide.

In these experiments, the EWP power was characterized by the pressure p_{RE} under which the rheological explosion (RE) occurs. The upper boundary of the absorbed energy was estimated from the formula

$$E = Vp_{RE}^2/(2M), \qquad (1)$$

where M is Young's modulus of steel, and V is the volume of the wave guide. Inserting the experimental parameters ($V = 3.17 \cdot 10^{-6}$ m^3, p_{RE} = 5—30 kbar) and the known value $M = 2 \cdot 10^{11}$ Pa into Eq. (1), we obtain E = 2—72 J. Since the sample weight is usually equal to ~80 mg, we find that under the EWP action, the dose of unity action is 25—900 J g^{-1}, and the power is $1.25 \cdot 10^6$—$4.5 \cdot 10^7$ W g^{-1}.

Radicals and radical pairs

The EWP action on a mechanical mixture of PbO_2 with sterically hindered phenols results in the formation of the corresponding phenoxyl radicals.[12]

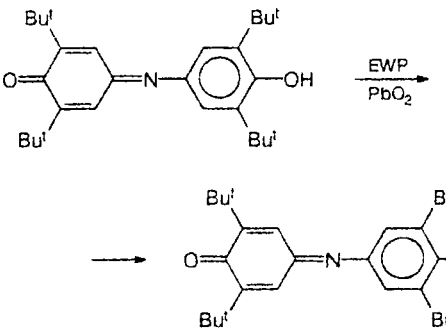

(2)

Under the same conditions, 3,6-di-*tert*-butyl-*o*-benzoquinone (Q) adds to silicon tetra-*tert*-butylbispyrocatechol to form silicon-containing biradicals.

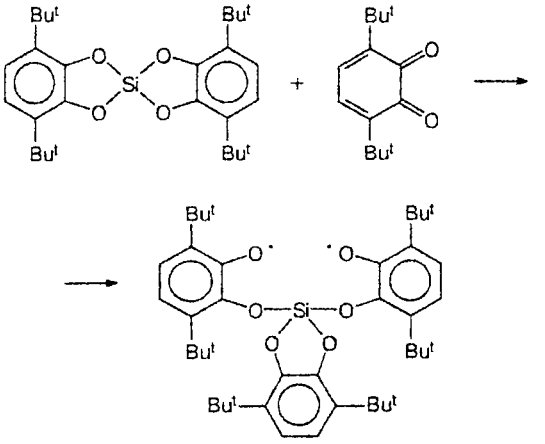

(3)

In the ESR spectra, the parameters of zero splitting of these biradicals (D = 30.0 mT, E = 2.3 mT) coincide completely with D and E values obtained for the interaction of the starting reagents in a solution and detected at 77 K.[23]

For simplicity, hereinafter we will use the following designations:

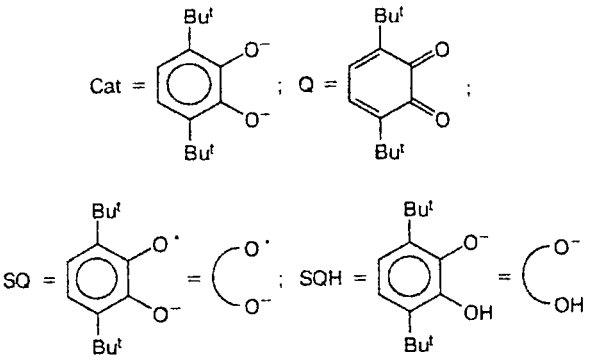

Under the EWP action on a mixture of Q and 3,6-di-*tert*-butylpyrocatechol (QH_2), radical pairs (RP) with D = 28.6 mT are formed.[12]

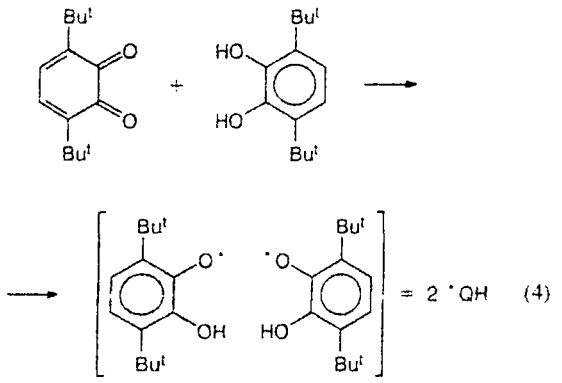

Thus, electron and proton transfer processes occur under the EWP action on solid organics.[12]

It has been shown[12–15] that RP with almost the same D and E parameters are formed upon the EWP action on a mechanical $Q+QH_2$ mixture and combined $Q+QH_2$ crystals that obtained from toluene solutions of these compounds (Table 1). In both cases, the formation of semiquinone radicals and RP has a threshold character (see Table 1, Fig. 1), and the yields of these particles at the threshold pressure p_{thr} (*i.e.*, at p_{RE}, after which no increase in the concentration of particles formed is observed) and the depth of chemical transformation for combined crystals are higher (see Table 1). This indicates that the EWP action on the mechanical $Q+QH_2$ mixture results in dispersion and mixing of these compounds leading to mixed associates of reagent molecules, ultrafine clusters consisting of hydrogen-bonded complexes and containing paramagnetic products.[14]

It has previously been established[24] that during photochemical reduction of sterically hindered *o*-benzoquinones by phenols in frozen solutions, the phototransfer of a hydrogen atom occurs to form the corresponding phenoxyl radicals as radical pairs. In this

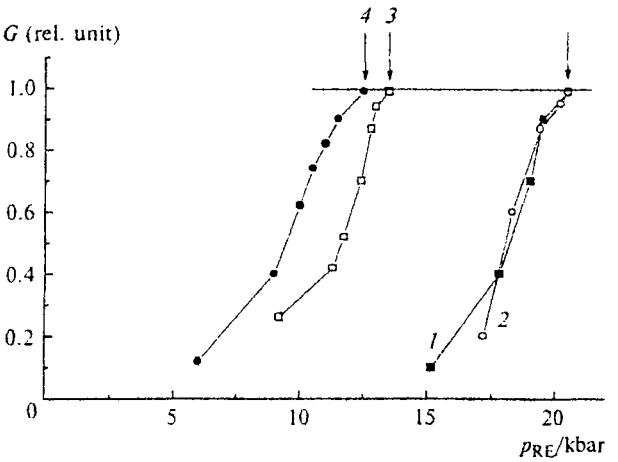

Fig. 1. Dependences of the relative yield (G) of radical pairs on p_{RE} value: *1*, in the $Q+QH_2$ mechanical mixture (1 : 1); *2*, in $Q+QH_2$ combined crystals (1 : 1); *3*, in the $Q-QH_2-PS$ system (45 : 45 : 10); and *4*, in the $Q-QH_2-PE$ system (30 : 30 : 40). Hereinafter in figures the threshold pressure (p_{thr}) is marked with arrows.

situation, an efficient spin-spin interaction of unpaired electrons occurs, which is observed by the appearance of lines with fine structure characteristic of molecules in the triplet state. Therefore, the mechanism of formation of radical products was studied in detail[13] for the $Q+QH_2$ mixture and a poor reducing agent, sulfur. The yields of radicals and RP upon EWP action on this system were determined. It was found that sulfur radicals ($g_{\parallel} = 2.225$, $g_{\perp} = 2.071$) are formed along with RP. In addition, a series of monoradical QH$^{\cdot}$ products is observed with a g factor of 2.0018 (when toluene was added into ampules with samples and ESR spectra were recorded at 300 K). The formation of radical products in this system has a threshold character, and the p_{thr} value de-

Table 1. Threshold pressures of EWP (p_{thr}), mechanochemical yields (G), depths of chemical transformations (α), concentrations (N), and geometric (r) and spectral (D) parameters for $Q+QH_2$, $Q+QH_2$+polymer systems

System	Radicals				Radical pairs [a]					
	p_{thr} /kbar	G at p_{thr} (particles /100 eV)	α	N /radical g^{-1}	p_{thr} /kbar	G at p_{thr} (particles /100 eV)	α	N /pairs g^{-1}	D /mT	r /Å
$Q+QH_2$ [b]	14	0.05	0.002	$5 \cdot 10^{18}$	20	0.03	0.004	$6 \cdot 10^{18}$	28.6	4.6
$Q+QH_2$ [c]	14	0.21	0.001	$2.4 \cdot 10^{19}$	20	0.056	0.008	$1.1 \cdot 10^{19}$	28.0	4.63
$Q+QH_2+PS$ [d] (45 : 45 : 10)	10	0.34	0.011	$9 \cdot 10^{18}$	13	$[0.016]_1$ $[0.08]_2$	$[0.002]_1$ $[0.01]_2$	$[7 \cdot 10^{17}]_1$ $[3.5 \cdot 10^{18}]_2$	$[7.0]_1$ $[28.0]_2$	$[7.35]_1$ $[4.69]_2$
$Q+QH_2+PE$ [e] (30 : 30 : 40)	8	0.2	0.196	$1.4 \cdot 10^{19}$	12	$[0.015]_1$ $[0.027]_2$ $[0.06]_3$	$[0.004]_1$ $[0.007]_2$ $[0.017]_3$	$[1.6 \cdot 10^{18}]_1$ $[2.7 \cdot 10^{18}]_2$ $[6.1 \cdot 10^{18}]_3$	$[4.7]_1$ $[12.0]_2$ $[24.5]_3$	$[8.39]_1$ $[6.14]_2$ $[4.84]_3$

[a] The data for RP with different distances between radicals are presented in brackets.
[b] Mechanical mixture.
[c] Combined crystals.
[d] PS is polystyrene.
[e] PE is polyethylene.

pends on the introduction of sulfur to the initial components.[13] The yields of sulfur radicals and semiquinone radicals ($QH^{\cdot}$) and RP are characterized by an antiparallel dependence at some ratios of S, Q, and QH_2 (Fig. 2): with an increase in the amount of sulfur, the concentration of $QH^{\cdot}$ radicals and RP first increases and then decreases. Based on this, we may suggest[13] the existence of competing reactions when EWP act on the system and propose a scheme of the process that includes electron transfer, probably, in the form of a quasi-particle e_q^-:

$$Q + QH_2 + S \xrightarrow{EWP} \longrightarrow e_q^- + H^+ + \text{radical products}, \quad (5)$$

$$e_q^- + Q\ (QH_2) \longrightarrow SQ\ (SQH), \quad (6)$$

$$e_q^- + S \longrightarrow S^{\cdot -}. \quad (7)$$

The experiments performed made it possible to propose the following convection mechanism[14] of the mechanochemical reactions under the EWP action. When the pressure increases in a closed volume in which the sample is placed, processes of nucleation of dislocations and structural heterogeneities (micropores or regions with elevated density) occur there. When the pressure decreases sharply, dislocations begin to move, adjacent layers are displaced, and variable elastic strains (oscillation processes, acoustic emission[25]) that weaken chemical bonds and destroy the solid lattice appear. These phenomena result in the formation of electrons and charged and ultrafine particles (UFP) with a metastable surface, which induce chemical reactions. This situation agrees with the experimental data considered above but requires refinement and specification.

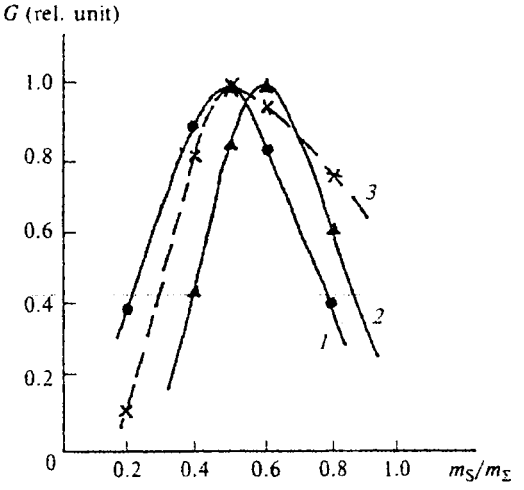

Fig. 2. Dependences of the relative yield (G) of radical pairs (*1*), oxyphenoxyl radicals (*2*), and radicals of elemental sulfur (*3*) in the $Q+QH_2+S$ mixture on the mass fraction of sulfur (m_S/m_Σ).

Comparison of the data of X-ray diffraction phase analysis (XRD) of mechanochemical mixtures and the kinetics of formation of free radical and triplet paramagnetic centers showed that processes of electron and proton transfer become possible only after deep dispersion of a mixture, when a long-range order is absent from the crystalline lattice.[14]

Deformations due to mechanical strains already occur in the scale of intermolecular distances and result in the cleavage of the hydrogen bonds in QH_2 complexes to form a pair of semiquinone radicals, probably, by reactions (8) and (9).

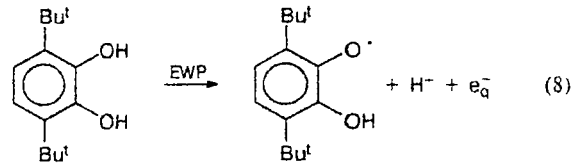

(8)

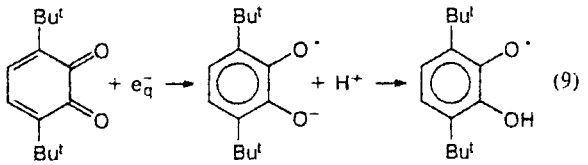

(9)

Ultrafine particles that appear under the EWP action consist of Q and QH_2 structurally differ from combined $Q+QH_2$ crystals grown from a toluene solution, and paramagnetic products are stabilized in them for a long time (several weeks at room temperature). In fact, the study of products of low-temperature (77 K) photolysis of glassy $Q+QH_2+PS$ samples ($Q : QH_2 : PS = 45 : 45 : 10$) subjected to EWP showed that the intensity of ESR signals of radical pairs with $D_1 \approx 7.0$ mT and with $D_2 \approx 28.0$ mT increases during photolysis (see Table 1). The ESR spectra of RP appearing during photolysis can be distinguished from those of mechanically generated RP only by stability and the sign of the D constant. These differences appear in strong magnetic fields at very low temperatures.[27,28] Therefore, the formation of photolytic RP is indicated only by an increase in the intensity of the spectrum recorded previously for RP generated by mechanochemical activation. This implies that the phototransfer of the hydrogen atom from pyrocatechol to quinone is not accompanied by structure deformation, which stabilizes the generated RP, or formation of free e_q^- and H^+.

Mechanoactivation leads to the formation of mixed crystals, because the XRD data indicate that the mixture is transformed into the amorphous state without appearance of new crystal structures. Thus, mixed crystals appear at a level of nanostructures, which are not detected by XRD, but are important for stabilization of free radical states.

All data presented confirm the assumption that the formation of free radical states in solid phase mecha-

nochemical reactions (2)—(9) is due to the dynamic component, EWP, rather than to the statistical deformation of the sample. In fact, it follows from the data presented in Table 1 that the solid matrix, in particular, PE or PS, participates in processes of elastic energy transport and dissipation, *i.e.*, affects both thresholds of formation of radicals and RP (see Fig. 1), their spectroscopic and geometric parameters, and the yield and depth of chemical conversion of Q and QH_2 (see Table 1).

Organometallic complexes

The proposed[14] convection model of mechanochemical reactions and the statement on the appearance of a free electron[13] under EWP action required a more detailed substantiation and further development with the use of various solid state reagents. Therefore, the reactions of some II—IV Group metals (Zn, Cd, Al, Ga, In, Sn, Pb, Bi) with Q under the EWP action were studied[16] to elucidate the possibility of mechanochemical synthesis of semiquinolate complexes of these metals in the mono-, bi-, and triradical states. All samples were treated with EWP at a pressure of 10 kbar. Primarily the ESR spectra of the products exhibited only singlet lines (Fig. 3, spectrum *1*), whose parameters are presented in Table 2. To identify the paramagnetic complexes formed, the reaction products that arose after the EWP treatment were extracted with toluene and studied by ESR at 300 and 77 K. Analysis of the ESR spectra obtained at 77 K for toluene solutions (see Fig. 3, spectra *2*—*5*) showed[16] that $M(SQ)_3$ triradicals in the quartet state are formed in the case of Al, Ga, and In; for Zn, Sn, and Pb, biradicals $M(SQ)_2$ with two semiquinolate ligands are formed; and Tl and Bi give monoradical Tl(SQ) and Bi(SQ)Cat complexes. Only the characteristic spectrum of the $QH^{\cdot}$ radical is observed at 300 K in toluene solutions in the region of the *g*-factor of a free electron.

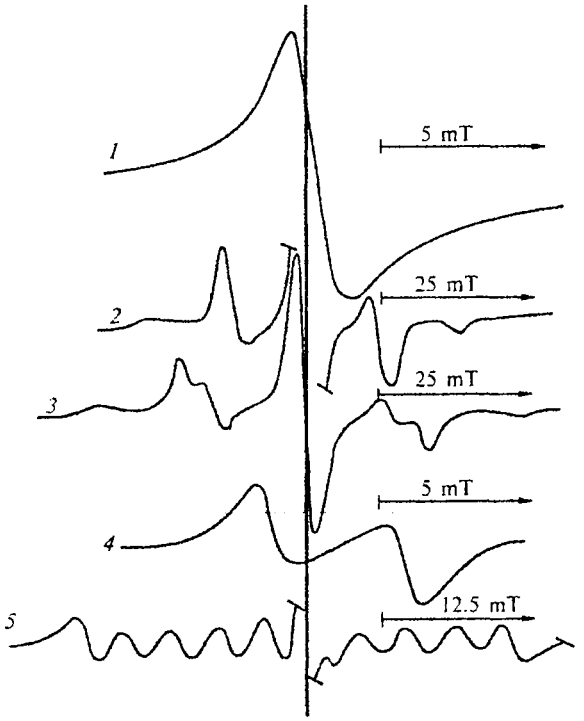

Fig. 3. ESR spectra: *1*, Q+Pb mixtures after EWP treatment (300 K); *2*—*5*, frozen (77 K) toluene extracts of Q+Ga (*2*), Q+Zn (*3*), Q+Tl (*4*), and Q+Bi (*5*).

Table 2. Spectral parameters (ΔH, *g*, and *D*), yields (G_1 and G_2), and depths of chemical transformations (α) of paramagnetic complexes after EWP treatment of the Q+M system

M	ΔH /mT	*g*	*D* /mT	G_1 particles/100 eV	G_2 particles/100 eV	α
Tl	14.0	2.0039	—	0.6	0.3	$3.5 \cdot 10^{-3}$
Zn	9.0	2.0027	−17.0	2.25	0.96	0.042
Cd	13.0	2.0028	—	5.1	2.5	0.1
Sn	23.0	2.0039	—	13.0	1.2	$7 \cdot 10^{-3}$
Pb	20.0	1.9998	—	1.8	1.4	$9 \cdot 10^{-3}$
Al	17.0	2.0046	14.0	3.8	0.67	0.036
Ga	10.0	2.0046	13.2	12.0	0.83	0.03
In	19.0	2.0028	6.0	50.4	11.8	0.4
Bi	45.0	1.9974	—	48.0	7.0	0.25

It should be emphasized that the mechanochemical synthesis of the complexes under consideration occurs during ~100 μs for metals with different melting temperatures. When a metal reacts with quinone, radical complexes are formed in the solid phase, probably, as exchange clusters, because only closely arranged radical products can give a singlet line due to intermolecular spin exchange. Therefore, information on the fine structure of spectra cannot be obtained for powdered samples. The formation of exchange clusters with a high effective spin ($S > 3/2$) is also indicated by the difference in yields *G* (the number of paramagnetic centers per 100 eV of the energy (particles/100 eV) inlet into the sample by EWP) for paramagnetic products as a powder (G_1) and in a toluene solution (G_2). In some cases, the G_2 values are substantially lower than G_1 (see Table 2).

Mechanochemical yields for different systems vary considerably. The character of the dependence of G_1 on the oxidation state of the metal (*Z*) in *o*-semiquinone radical complexes (Fig. 4) suggests that the yields in these heterogeneous solid state processes are determined by several factors, including, perhaps, rigidity of the crystalline lattice of the metal. As can be seen from the data in Table 2, the maximum yield is observed for the reaction of *o*-benzoquinone with In and Bi and then with Sn, Ga, Al, Cd, Zn, Pb, and Tl.

Probably, when an elastic wave pulse passes through a sandwich-like sample (metal—Q), the metal is activated at a high pressure due to deformation of the crystalline lattice and a considerable mobility at the interfaces. Since in the complexes obtained the ligand is

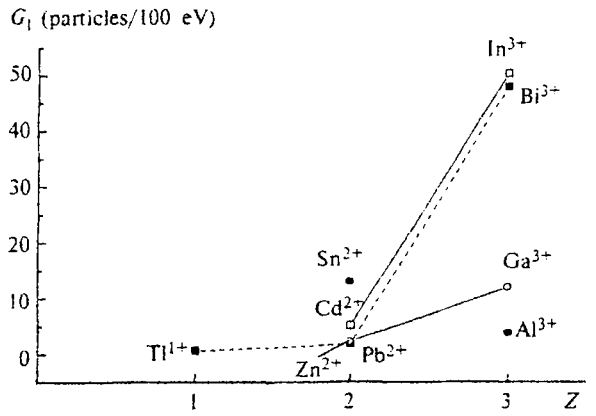

Fig. 4. Dependence of the yield (G) of semiquinone complexes on the oxidation state of the metal (Z) in the M—Q system.

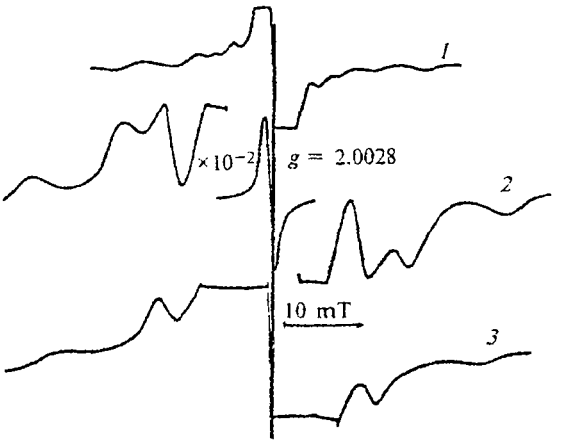

Fig. 5. ESR spectra of solid samples after EWP treatment on system I with ZnO (*1*), Al_2O_3 (*2*), and ZrO_2 (*3*).

negatively charged and the metal atom is positive (both initial compounds contain no ions), at the first stages an electron is most likely transferred from the metal surface to quinone. This is confirmed by the fact that the yields of the mechanochemical reactions correlate, in most cases, with the oxidation state of the metal in the complex formed (see Fig. 4). The rate of formation of metal-radical complexes in this stage is mainly controlled by the molecular mobility and chemical reactivity of reagents rather than mechanical properties of starting powders.

Thus, the probable mechanism of the process includes reactions (10)—(12)

$$M \xrightarrow{EWP} Ze_q^- + M^{Z+} \qquad (10)$$

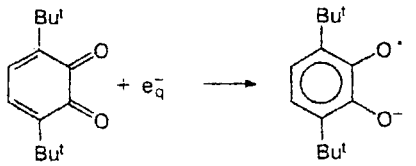

(11)

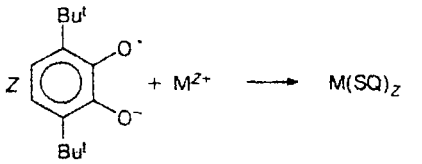

(12)

These concepts have been developed in Ref. 17 for mechanochemical synthesis of metal-containing mono-, bi-, and triradicals during pulse mechanical treatment of mixtures of metal oxides (CuO, ZnO, CdO, PbO, Al_2O_3, Ga_2O_3, Sb_2O_3, Bi_2O_3, Cr_2O_3, TiO_2, GeO_2, ZrO_2, SnO_2) with quinone and pyrocatechol of different compositions: M_xO_y : Q : QH_2 = 40 : 1 : 1, M_xO_y : QH_2 = 20 : 1, M_xO_y : Q = 20 : 1 (hereinafter, systems I, II, and III, respectively).

After EWP action on systems with CuO, the ESR spectra of solid state samples exhibit a characteristic signal with $a_\perp$ = 4 mT and $a_\parallel$ = 18 mT with anisotropic HFS on ^{63,65}Cu nuclei. Other MO oxides are characterized by either single lines with the g-factor close to g_e or (for the (ZnO, CdO)+(Q+QH_2) systems) a fine structure corresponding to $M(SQ)_2$ biradicals[23] (Fig. 5).

After the EWP treatment of (Al_2O_3, Ga_2O_3)+QH_2, (Q+QH_2), the ESR spectra of systems with M_2O_3 contain, along with single lines, a fine structure in the region of g_e (see Fig. 5), which is characteristic of the $(QH)M^{3+}(SQ)_2$ biradical.[23] In the case of the Bi_2O_3 systems with QH_2 and (Q+QH_2), two lines are observed: one line with ΔH = 0.5 and 1.5 mT and another line with ΔH = 16 and 17 mT, which probably belong to $Q^{\cdot -}$ and CatBi(SQ) particles.

The spectra of the systems with MO_2 also contain single lines in the region of g_e and the fine structure in the (TiO_2, SnO_2, ZrO_2)+QH_2 (Q+QH_2) and GeO_2+Q (Q+QH_2) systems characteristic of particles of the $CatM^{4+}(SQ)_2$ type[23] (see Fig. 5).

In the spectrum of system III, only a narrow singlet in the region of g = 2.00 can be detected, and its intensity is much lower than that of the ESR signals in systems I and II after EWP treatment.

In the solid state, HFS of an intense narrow signal in the region of g = 2.00 cannot be resolved. In addition, more convincing arguments are necessary to confirm that the EWP action results in the formation of biradical particles and, probably, triradicals. For this purpose, ESR spectra were recorded for the products extracted with toluene from solid state samples (at 300 and 77 K) and of evacuated precipitates after removal of toluene-soluble products of mechanochemical reactions (at 300 K). The following species were found in solutions of systems I and II at 300 K (the ESR spectra of some of them are presented in Fig. 6): for ZnO, CdO, and PbO, (SQ)M(SQH) (M = Zn, Cd, Pb) and $Pb(SQ)_2$;

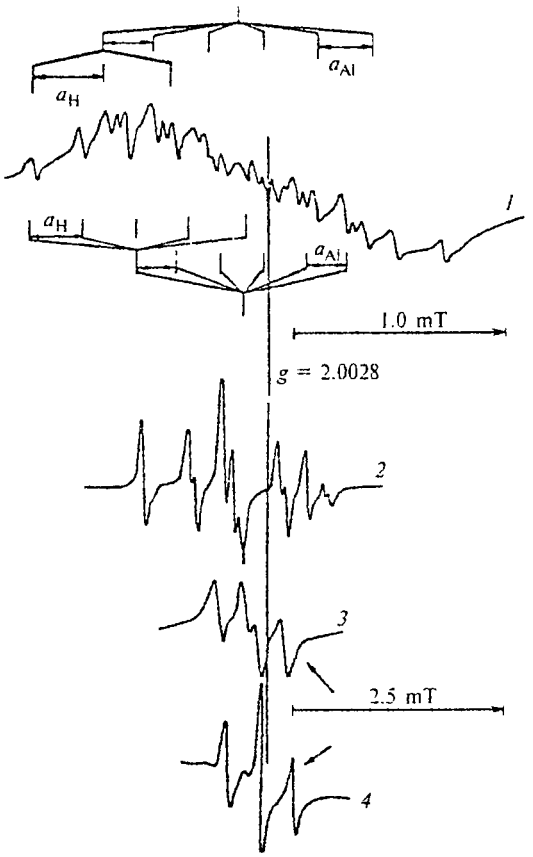

Fig. 6. ESR spectra of toluene solutions (300 K) of the products of mechanochemical reactions with Al_2O_3 in system I (*1*), with GeO_2 in system II (*2*), with ZrO_2 in systems I and III (*3*), and ZrO_2 in system II (*4*).

for Al_2O_3, CatAl(SQ) (sextet of quintiplets) and (SQH)Al(SQH)$_2$ (sextet of triplets); for Cr_2O_3, $[CrQ_3]^{\cdot+}A^-$ (A^- is, *e.g.*, OH^-); and for Bi_2O_3, CatBi(SQ) (a spectrum of ten lines).

The CatSb(SQ) complex (multiplet due to the interaction of an unpaired electron with antimony isotopes ^{121}Sb (J = 5/2) and ^{123}Sb (J = 7/2)) is formed in system II with Sb_2O_3, and the (Cat)$_2$Sb(SQ) complex is formed in the Sb_2O_5+Q (QH_2+Q) systems.[23]

Two species, (SQ)GeOHCat and (SQ)Ge(SQH)Cat, are observed at 300 K in a solution of system II with GeO_2 (see Fig. 6), and only one species, (SQ)GeOHCat, is formed in the GeO_2+Q+QH_2 system.

In the case of SnO_2, the (SQ)Sn(SQH)Cat species (triplet from equivalent protons (SQ) with splitting on $^{117,119}Sn$ nuclei) is detected at 300 K in a solution of the system with Q+QH_2 only.

At 300 K, the solutions of systems I and II with TiO_2 contain a radical of the (SQ)TiO(SQH) type (doublet of doublets from nonequivalent protons in SQ and HFS from ^{47}Ti (J = 5/2, 7.28%) and ^{49}Ti isotopes (J = 7/2, 5.51%), $\mu(^{47}Ti) = \mu(^{49}Ti)$).

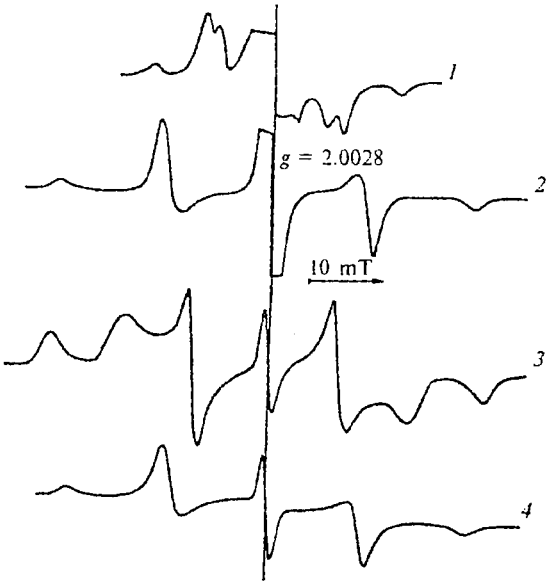

Fig. 7. ESR spectra of frozen (77 K) toluene solutions of the products of mechanochemical reactions in systems I and II with ZnO (*1*), Al_2O_3 (*2*), ZrO_2 (*3*), and TiO_2 (*4*).

The ESR spectrum of the ZrO_2—QH_2 system in a solution exhibits a triplet from (SQ)ZrO(SQH) and a doublet of doublets from (SQ)Zr(SQH)Cat in the ZrO_2+Q+QH_2 system.

The ESR spectra corresponding to the (Zn, Cd)(SQ)$_2$ biradicals, Al(SQ)$_3$ and Ga(SQ)$_3$ triradicals, and Cat(Sn, Ge, Zr)(SQ)$_2$ and (Ti, Zr)O(SQ)$_2$ biradicals were recorded at 77 K (in frozen toluene solutions) in systems I and II (Fig. 7).

Thus, only three new species, which have not been obtained by traditional methods, were found in the study of the EWP treatment of the systems considered:

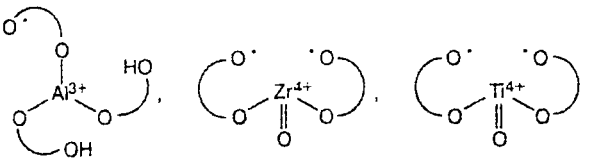

For the (SQ)(Zr, Ti)O(SQH) species, E = 0, *i.e.*, two electron states of three states become degenerate in the zero field, due to the specific features of their structure.

All surface sites were observed at 300 K. For all oxides, excluding CuO, Al_2O_3, and Ga_2O_3, only singlet lines were observed, which are probably attributable to species of the type

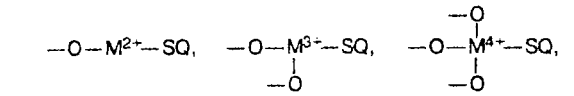

where the fragments

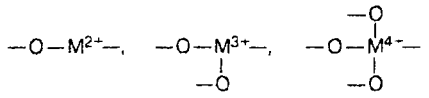

belong to solid oxide.

On the oxide surface in the systems with CuO, CatCu species appear, and the systems with Al_2O_3 and Ga_2O_3 exhibit species of the 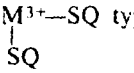 type.

In all cases, the ratio of the concentration of surface sites to the concentration of extracted products is equal to 10^{-2}—10^{-3}, *i.e.*, under EWP action, the concentration of surface sites formed is 2—3 orders of magnitude lower than that of other products.

Thus, it follows from the previously published experimental data[17] that after EWP treatment solid samples contain a series of mono-, bi-, and triradicals. Depending on the type of oxide (MO, M_2O_3, or MO_2), surface complexes on oxides (mono- and biradicals) and a new solid phase, which are the products of chemical reactions, are formed. In the solid phase, molecular products are united to form exchange clusters and decompose to individual mono-, bi-, and triradicals only in toluene solutions (this concerns monoradicals of all oxides considered and the $Cu(SQH)_2$ species, as well as biradicals in the case of ZnO, CdO, TiO_2, GeO_2, ZrO_2, and SnO_2 and triradicals in the case of Al_2O_3 and Ga_2O_3). A similar situation was observed when the metal—Q systems were treated with EWP.

We calculated the yields (G) of solid organometallic compounds (for all particles formed in the solid state and for each oxide present in the sample) produced upon the EWP action on systems I, II, and III and the depth of chemical transformation (α) of initial Q and QH_2 (Table 3). As in the case of the metal—Q system, the G values change with an increase in the oxidation state Z of the corresponding metal in the period (Fig. 8). Therefore, the formation of radical products is affected by the activity of oxides (related to the position of the corresponding metal in the periodic system of elements) and

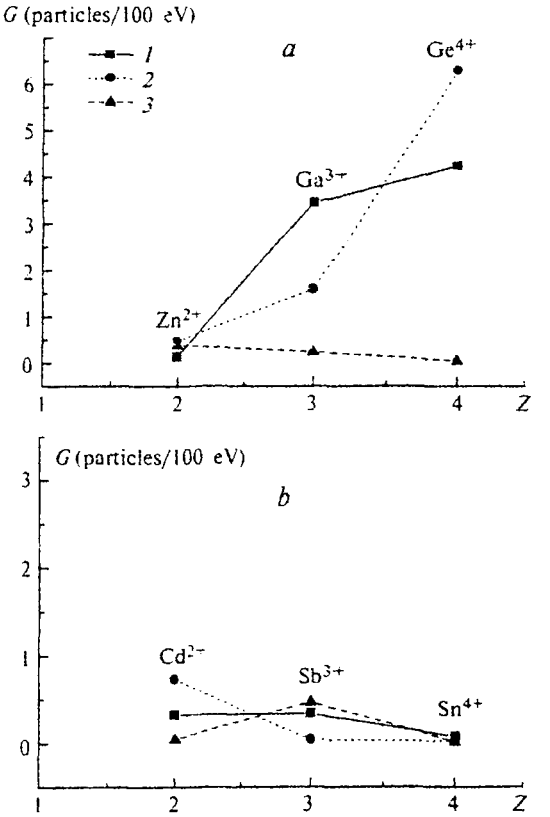

Fig. 8. Changes in the yields (G) of metal semiquinone complexes in systems I (*1*), II (*2*), and III (*3*) at different oxidation states (Z) of metals of the IV (*a*) and V (*b*) Periods.

Table 3. Mechanochemical yields (G (particles/100 eV)) and depths of chemical transformations (α) of Q and QH_2 in M_xO_y+Q+QH_2, M_xO_y+QH_2, and M_xO_y+Q systems

Oxide	M_xO_y+Q+QH_2 (40 : 1 : 1)		M_xO_y+QH_2 (20 : 1)		M_xO_y+Q (20 : 1)	
	G	α	G	α	G	α
Al_2O_3	3.59	0.48	0.62	0.16	2.1	0.36
TiO_2	0.48	0.06	0.07	0.0126	0.23	0.0124
Cr_2O_3	0.047	0.005	0.004	$1.65 \cdot 10^{-3}$	0.034	0.08
CuO	0.29	0.092	0.12	0.038	0.06	0.019
ZnO	0.135	0.007	0.46	0.063	0.38	0.053
Ga_2O_3	3.45	0.6	1.59	0.12	0.24	0.04
GeO_2	4.24	0.68	6.3	0.54	0.044	0.01
ZrO_2	3.0	0.2	1.0	0.05	0.043	0.0135
CdO	0.33	0.017	0.73	0.022	0.048	0.014
SnO_2	0.076	0.014	0.023	$4.26 \cdot 10^{-3}$	0.014	0.0032
Sb_2O_3	0.34	0.133	0.042	0.024	0.47	0.122
PbO	0.24	0.03	0.1	0.035	0.039	0.014
Bi_2O_3	1.6	0.087	0.54	0.33	0.006	0.0024

the redox ability of other reagents (Q, QH_2). In fact, for the $ZnO—Ga_2O_3—GeO_2$ and $CdO—Sb_2O_3—SnO_2$ series, on going from the M_xO_y+Q to M_xO_y+QH_2 system, a distinct tendency for increasing the yields of products by 1—2 orders of magnitude is observed (see Table 3 and Fig. 8). For the M+Q systems, the G values are much higher than those for the M_xO_y+Q systems with the same metal.

In heterogeneous catalysis,[18] similar dependences are related to so-called Lewis acidic sites, which are coordinationally unsaturated metal ions on oxide surfaces. Similar sites interact, as a rule, with electron donors. A considerable number of acidic sites appear on the oxide surface upon the EWP action. This agrees well with the data in Ref. 4, in which the catalytic activity of the oxide surface is shown to increase due to the shift of dislocations upon this mechanical treatment on this surface. This results in the rearrangement of chemical bonds and charge relaxation on the surface of the initial oxide. According to the dislocation theory,[4] about 70% of the surface atoms can be transformed into the active state, because they are in the zone of action of elastic distortions around dislocations emerging to the surface.

Probably, free e^- and H^+ are formed when dislocations emerge to the oxide surface. Free electrons can react with metal ions in oxides *via* the reactions

$$M^{Z+} + e^- \longrightarrow M^{(Z-1)+} \qquad (13)$$

or with Q *via* reaction (6), resulting in SQ. Protons react with O^- ions, which are present on the oxide surface (or appear due to EWP), to form surface OH groups. Then metal atoms or fragments of the MOH lattice, which are weakly bound to the oxide surface, are mechanically removed and react with SQ and SQH radicals and Q and QH_2 molecules, which is most probable from the viewpoint of formation of final (detected by ESR) products. Both external EWP and surface elastic waves that appear when dislocations emerge to the oxide surface are responsible for the intense removal of species from the surface of initial solid state components. Thus, the experimental results[17] make it possible to assume that the proposed[14] convection model adequately describes solid state chemical reactions under the EWP action.

The EWP action initiates electron and proton (or hydrogen atom) transfer processes, chemical bond cleavage, and removal of atoms of fragments of the surface of solid state reagents. This is confirmed in Ref. 18, in which solid state reactions of $Cr(CO)_6$, $Mo(CO)_6$, $W(CO)_6$, and $Mn_2(CO)_{10}$ with Q in molded mixtures of (carbonyl+Q) powders occur under the EWP action. Paramagnetic semiquinone complexes of Cr, Mo, and W are the products of reactions of Q with $Cr(CO)_6$, $Mo(CO)_6$, and $W(CO)_6$.

An ESR signal with the linewidth ΔH = 1.5 mT and g_{aver} = 1.973 is observed in the spectrum of the solid state after the EWP action on $Cr(CO)_6$+Q mixtures (1 : 1, w/w). When EWP act on mixtures of $Mo(CO)_6$+Q and

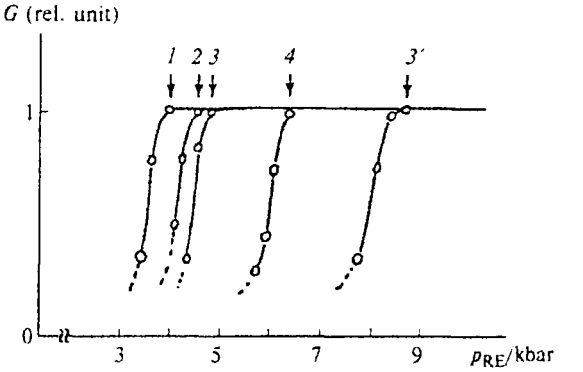

Fig. 9. Dependences of the relative yield (G) of paramagnetic products on p_{RE}: *1*, $Cr(CO)_6$+Q (1 : 1); *2*, $Mo(CO)_6$+Q (1 : 1); *3*, *3'*, $Mn_2(CO)_{10}$+Q (1 : 1) (for binuclear (*3*) and mononuclear (*3'*) complexes); and *4*, $W(CO)_6$+Q (1 : 1).

$W(CO)_6$+Q (1 : 1) powders, singlet lines with ΔH = 1.2 and 2.1 mT, g_{aver} = 2.0046 and 2.0036 ($g_\perp$ = 2.0124, $g_\parallel$ = 1.9992), respectively, are also observed.

An additional signal with ΔH = 1.7 mT and g_{aver} = 2.0025 appears when EWP with p_{RE} = 4—5 kbar act on a mixture of $Mn_2(CO)_{10}$+Q (1 : 1) powders. When the EWP power increases in the region of p_{RE} = 9—10 kbar, the intensity of this broad signal decreases, and a six-component signal appears against its background due to HFC with the nucleus of one Mn atom.

It is established that all these paramagnetic centers to which the detected singlet ESR signals are attributed appear at different threshold energies of the EWP action. For example, for chromium, molybdenum, tungsten, and manganese complexes, p_{thr} = 4.0, 4.6, 6.5, and 4.8 kbar, respectively, and the G values (at p_{thr}) are 0.115, 0.054, 0.014, and 0.046, respectively (Fig. 9). The mechanochemical yields of all complexes obtained are sufficiently low, and in the series of chromium, molybdenum, and tungsten carbonyls they decrease as the number of the period increases.

Since all newly found signals attributed to species appearing under EWP cannot also be resolved in the solid state due to strong exchange interaction, extraction with toluene was used to identify these species. After this procedure, signals with resolved HFS structure appear in ESR spectra. For example, after dissolution of the preliminarily EWP-treated $Cr(CO)_6$+Q mixture in toluene, the ESR spectrum of the cation of the chromium tris-*o*-semiquinone complex is observed. An unpaired electron interacts with six equivalent protons of three 3,6-di-*tert*-butyl-*o*-semiquinone ligands (a_H = 0.085 mT) and the magnetic ^{53}Cr isotope (a_{Cr} = 2.55 mT), g_{aver} = 1.9690. This result allows one to assert that the following reaction occurs in the solid state under the EWP action:

$$3\,Q + Cr(CO)_6 \xrightarrow[-6\,CO]{} [CrQ_3]^{\cdot+}A^-. \qquad (14)$$

It is most likely that OH^-, which can be present in toluene in microadmixtures, is the A^- anion.

The following species were observed when EWP-treated $Mo(CO)_6$+Q and $W(CO)_6$+Q (1 : 1) powders were dissolved in toluene:

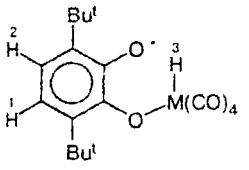

M = Mo, W.

For the molybdenum complex, g_{aver} = 2.0035, $a_{H(1)}$ = 0.55 mT, $a_{H(2)}$ = 0.2 mT, and a_{Mo} = 0.15 mT; and for the tungsten complex, g_{aver} = 2.00, $a_{H(1)}$ = 0.65 mT, and $a_{H(2)}$ = 0.13 mT. In the case of M = Mo, the ESR spectra differ from those of the radical formed during the photochemical reaction[29] and recorded in toluene at −60 °C ($a_{H(1)}$ = 0.38 mT, $a_{H(2)}$ = 0.30 mT, $a_{H(3)}$ = 0.016 mT, and a_{Mo} = 0.1937 mT).

The most sharp distinctions in the structure of paramagnetic species obtained upon EWP action and that of the previously known species were observed for the reaction of $Mn_2(CO)_{10}$ with Q. In fact, UV radiation induces the $\cdot Mn(CO)_5$ radical[23] to add to *o*-quinone to form the manganese-containing *o*-semiquinone complex.

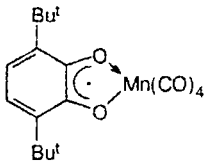

Species of two types appear when EWP acts on the Q+$Mn_2(CO)_{10}$ system, depending on the EWP power.

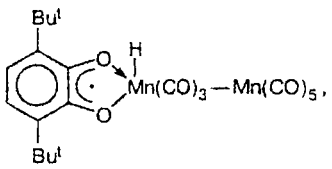

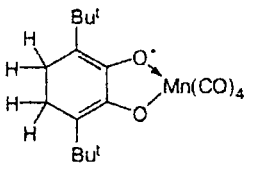

After the EWP action at p_{RE} = 4.8 kbar and dissolution of the products in toluene, their ESR spectrum exhibits a signal of a binuclear manganese complex corresponding to the interaction of an unpaired electron with two equivalent protons of the *o*-semiquinone ligand and two nonequivalent ^{55}Mn nuclei (a_H = 0.325 mT, $a_{Mn(1)}$ = 0.5 mT, $a_{Mn(2)}$ = 0.225 mT) (Fig. 10). With EWP action at p_{RE} ≈ 10 kbar, an ESR signal of a mononuclear complex is observed in the form of a sextet in which each line on the manganese nuclei (a_{Mn} = 0.6 mT) is split to five lines with binomial distribution of intensities with a splitting value of 0.325 mT typical of SQ [17] (see Fig. 10).

The experimental results[16–18] presented above show that EWP treatment makes it possible to perform chemical reactions *via* new and unusual channels, and the yields of the products of these reactions depend on the nature of metal and have a threshold character.

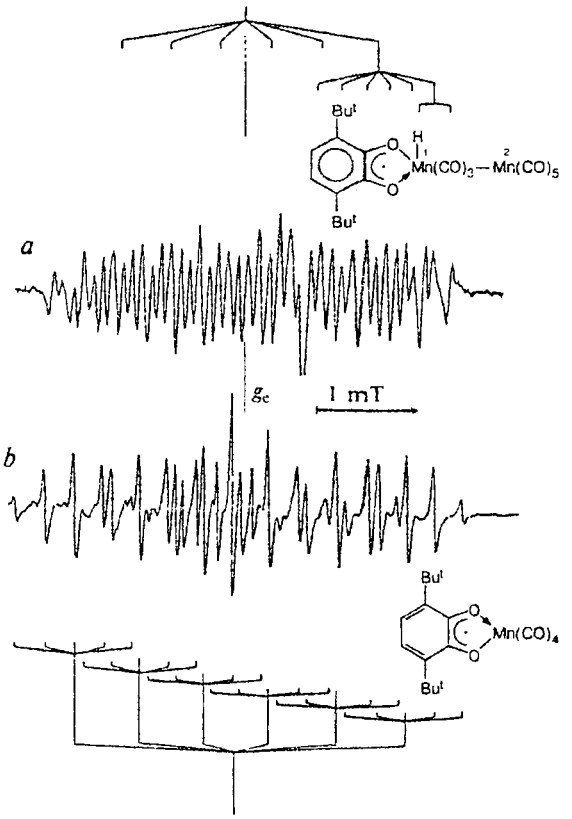

Fig. 10. ESR spectra of toluene solutions of a mixture of powders $Mn_2(CO)_{10}$+Q (1 : 1) after EWP action at p_{RE} = 4.8 kbar (*a*) and 10 kbar (*b*).

Ultrafine metal particles

The majority of works considered above concern the problems of mechanochemical synthesis of organometallic complexes. An inverse problem is also of interest: to destruct organometallic compounds under EWP with the purpose of extracting coordinated metal atoms.

The decomposition of cyclopentadienyl-π-(3)-1,2-dicarbolyliron(III) ($CpFe^{3+}(C_2B_9H_{11})$, **1**) and cyclopentadienyl-π-(3)-dicarbolylcobalt(III) ($CpCo^{3+}(C_2B_9H_{11})$,[5] **2**) in the presence of a weak reducing agent, elemental sulfur or sulfur-containing copolymer (CP) of tetrafluoroethylene and perfluoro-4-methyl-3,6-dioxa-7-octene-1-sulfanyl fluoride (CF_2=CF—O—CF_2—*CF*(CF_3)—O—CF_2—SO_2F),[19] has been studied.[19] The copolymer has a comb-shaped structure and contains ~12 mol.% second comonomer. This CP was chosen because lateral branches with the corresponding terminal functional groups form nanoclusters in which diffusion processes are substantially facilitated as compared to those in the perfluorinated matrix.

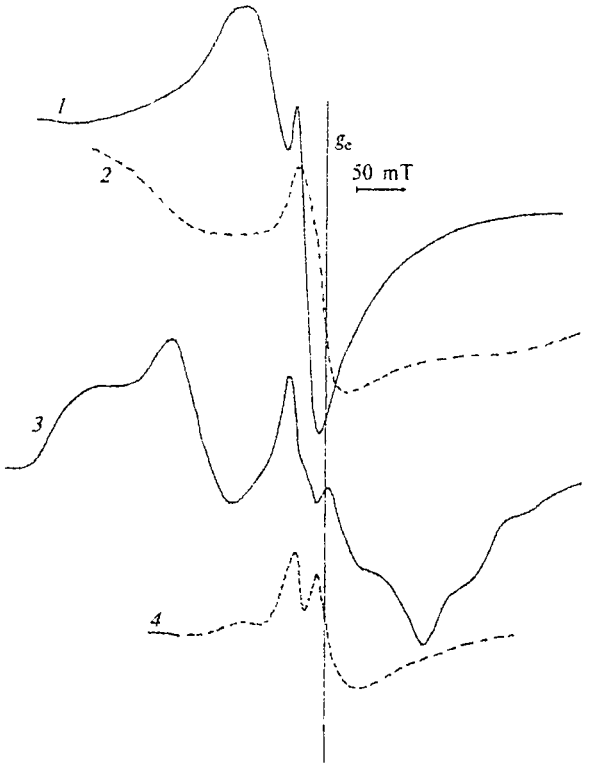

Fig. 11. FMR spectra of the products of pulse mechanical treatment of mixtures of powdered complexes **1** and **2** with elemental sulfur with weight ratios of initial components **2** : S = 1 : 1 (*1*), **1** : S = 1 : 1 (*2*), and CP—(**2**+S), **2** : S = 1 : 1 (*3*), and CP—(**1**+S) samples, **1** : S = 1 : 1 (*4*).

It has been established that the EWP treatment of mixtures of complexes **1** and **2** with elemental sulfur results in their decomposition and formation of the metal followed by its aggregation to form Fe_m or Co_m UFP, respectively. This follows from analysis of the ferromagnetic resonance (FMR) spectra, which exhibit two lines with g_{eff} = 2.17 and the linewidth ΔH = 35 and 100 mT for the **2**+S (1 : 1, hereinafter the ratios are given in weight fractions) mixture treated with EWP and one asymmetrical line with g_{eff} = 2.17 and ΔH = 40 mT for the **2**+S (2 : 1) mixture. In the case of the **1**+S mixtures with ratios of 1 : 1 and 2 : 1, FMR spectra with g_{eff} = 2.05 and 2.0, ΔH = 60 and 67 mT, respectively (Fig. 11), were observed.

The structure of the FMR spectra of CP—(**1**+S) and CP—(**2**+S) samples after the EWP action differs from that of the previous spectra (see Fig. 11): all of them occupy a wider magnetic field range due to superposition of several FMR lines with different widths. For the CP—(**2**+S) samples with the ratio **2** : S = 1 : 1, lines with widths of 35, 100, 250, and 350 mT were detected (see Fig. 11), and in the case of **2** : S = 2 : 1, lines with widths of 35, 100, and 250 mT were observed. The spectra of the CP—(**1**+S) samples with the ratios **1** : S = 1 : 1 and 2 : 1 exhibit lines with widths of 25, 65, 175 mT and 60, 175 mT, respectively.

Thus, the FMR spectra of particles which were injected in CP films differ by a great scatter over the line width and occupy the field range from zero to 500 mT.

Analysis of these data and those in Refs. 30 and 31, in which dependences between the FMR linewidth and UFP size are presented, suggest that the size distribution of cobalt UFP obtained falls in an interval of 1—13 nm. In the case of iron UFP, these correlations exist only for FMR lines with ΔH = 25—30 mT.[32]

It has previously[19] been concluded that iron(III) and cobalt(III) ions removed from complexes **1** and **2** undergo several successive reductions, and the polymeric matrix participates in the formation of iron and cobalt UFP.

Thus, the possibility of synthesizing ferromagnetic metal UFP under the EWP action was shown[19] for the first time, and a probable mechanism of their formation was suggested.

$$CpM^{3+}(C_2B_9H_{11}) \xrightarrow{EWP} M^{3+}, \quad (15)$$

$$2\,S \xrightarrow{EWP} S^{\cdot-} + S^{+}\ (S^{-} + e_q^-), \quad (16)$$

$$M^{3+} + n\,S^{\cdot-}\ (n\,e_q^-) \longrightarrow M^{2+}, M^{+}, M^{0}. \quad (17)$$

Then, according to the scheme of formation of metal UFP involving ions in unusual oxidation states,[32] particles of M_2^{3+}, M_2^{2+}, M_3^{2+}, *etc.* down to metal UFP are formed.

Rheological explosion

In all experiments described above, elastic wave pulses supplied to a sample through a steel wave guide were initiated by the rheological explosion of polymer plates in which elastic waves also propagate, *i.e.*, they are subjected to EWP. In this connection, it is interesting to elucidate: (1) which elastic waves are propagated in the polymer matrix during rheological explosion; (2) how do these elastic waves affect chemical processes in the polymer matrix containing metal ions?

It has been established[20] that two ensembles of Cu^{2+} complexes oriented at an angle of 90° to each other are formed under the rheological explosion of a sample consisting of two plates (molded $CuSO_4 \cdot 5H_2O$—PE, PP, PS). This indicates that Cu^{2+} penetrates into the polymer matrix due to diffusion related to longitudinal and transverse elastic waves that appear in the polymer matrix under rheological explosion.

To answer the second question, samples of solid polyepoxides obtained by mixing of polyethylenepolyamine (PEPA) and diane epoxide resin based on 4,4′-(2,2′-propylidenebisphenol) (ED-20) with volume

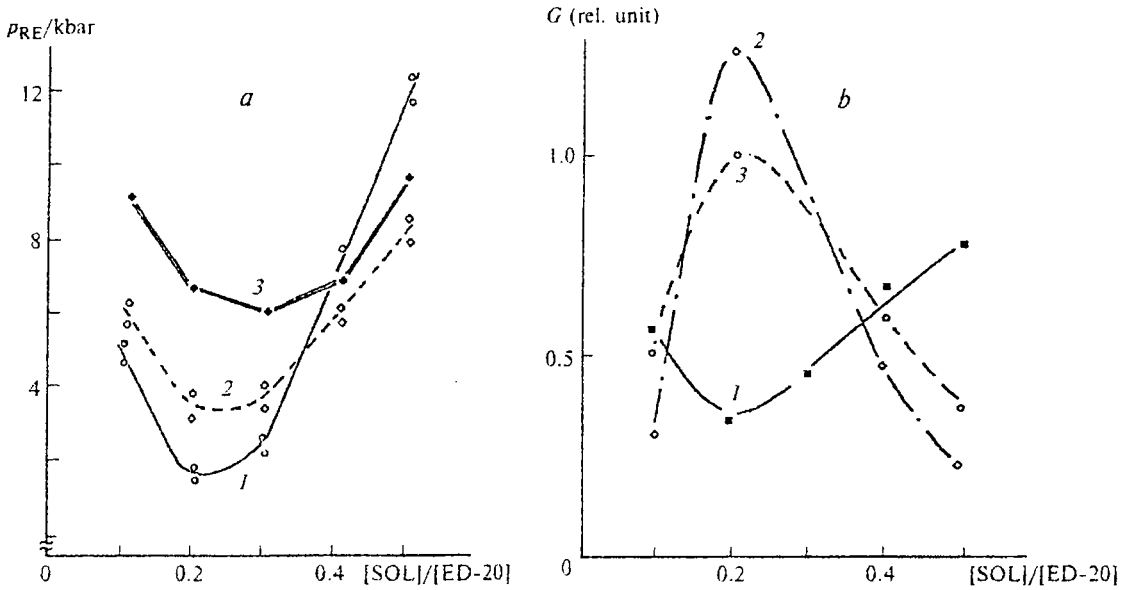

Fig. 12. Dependences of the rheological explosion pressure (p_{RE}) (*a*) and yields (*G*) of —O—Ar—$^{\cdot}CMe_2$ radicals (*b*) on the ratio [SOL]/[ED-20]: SOL = PEPA (*1*), PEPA+Ni^{II} complex (*2*), and PEPA+Co^{II} complex (*3*) (*G* = 1 corresponds to a concentration of 10^{18} radical g^{-1}).

ratios [PEPA] : [ED-20] = 0.1, 0.2, 0.3, 0.4, and 0.5 were studied.[21] Solidifiers (SOL) were 0.1 *M* solutions of Co^{II} and Ni^{II} acetates in PEPA, which were mixed with ED-20 in volume ratios [SOL] : [ED-20] = 0.1, 0.2, 0.3, 0.4, and 0.5. All samples were solidified in a thermostat at 100 °C for 8 h. The samples thus obtained, with a thickness of 1.0 mm and a diameter of 15 mm, were subjected to uniaxial compression, which was completed by rheological explosion, *i.e.*, the appearance of EWP directly in the polyepoxide. It was found that the pressure at which the rheological explosion occurs (p_{RE}) changes, depending on the amount of solidifier (PEPA or a solution of Co^{II}, Ni^{II} in PEPA) introduced into the ED-20 resin (Fig. 12, *a*). The p_{RE} values reach a minimum at the solidifier : resin ([SOL] : [ED-20]) ratio equal to 0.2—0.3. In the absence of metals, p_{RE} = ~2 kbar, and for Co^{II}- or Ni^{II}-containing polyepoxide, p_{RE} = 6 or 4 kbar, respectively. When the [SOL] : [ED-20] ratio increases or decreases, the pressures at which rheological explosion takes place increase reaching 6—10 kbar at [SOL] : [ED-20] = 0.1 and 8—14 kbar at [SOL] : [ED-20] = 0.5. It was assumed[21] that these dependences are related to the possibility of accumulating defects by the polyepoxide lattice, *i.e.*, relaxation properties of the lattice, which are determined by the polyepoxide structure: the more linkages are present (the maximum number of linkages appear at the ratio [SOL] : [ED-20] = 0.2—0.3), the more rapidly and the lower the pressure at which the critical concentration of defects is achieved. For an excess of a solidifier or resin in polyepoxides, the content of free terminal groups increases, the concentration of lattice units decreases, and the critical concentration of defects is accumulated at higher pressures. At the critical concentration, defects begin to interact with each other and migrate, which results in the appearance of an elastic wave propagating over the polyepoxide matrix.

The ESR study of all samples that underwent rheological explosion showed that only *para*-substituted dimethylbenzyl radicals (PDR) are formed in them. These radicals are stable at room temperature and appear due to homolytic cleavage of polyepoxide chains *via* the scheme

$$—O—Ar—CMe_2—Ar—O— \xrightarrow{EWP} \longrightarrow —O—Ar—\dot{C}Me_2 + \dot{A}r—O—, \quad (18)$$

Ar = 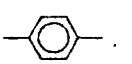 .

Thus, elastic waves result in the homolytic cleavage of polymer chains. Unstable phenyl radicals abstract hydrogen atoms from polymer chains. During this process, unstable alkyl radicals can also be formed and they decay due to "push-pull" electron transfer over polymer chains, which can lead to the formation of double bonds and molecular hydrogen. For polymers containing no metal ions, the yields of stable radicals change as follows: at the ratios [PEPA] : [ED-20] = 0.1 and 0.5, they are equal to 0.5 particles per 100 eV (the elastic wave energy was determined from the pressure in its front edge and frequency parameters), and at the ratio [PEPA] : [ED-20] = 0.2—0.3, they are 0.2 particles per 100 eV. In the case of Co^{II}- or Ni^{II}-containing polyepoxides, the dependence is inverse: at the ratios [SOL] : [Ed-20] = 0.1 or 0.5, the yields are about 0.15 particles per 100 eV, and for [SOL] : [ED-20] = 0.2—0.3,

about 1.2 particles per 100 eV. It follows from this that the chemical process includes stages in which metal ions act as acceptors of mobile reductive species, intermediate reagents.

It can be assumed that elastic waves appearing in polymer during rheological explosion interact with PDR and initiate the reversible process of removal of electron and proton to form olefin:

$$-O-Ar-\dot{C}Me_2 \overset{EWP}{\rightleftharpoons} \rightleftharpoons e_q^- + H^+ + -O-Ar-C(Me)=CH_2 \cdot \qquad (19)$$

In the presence of Co^{II} or Ni^{II} ions, which function as acceptors of e_q^-, the following competitive reaction can proceed:

$$Co^{II}\ (Ni^{II}) + e_q^- \longrightarrow Co^{I}\ (Ni^{I}), \qquad (20)$$

resulting in change in the dependence of the yields of PDR on the amount of solidifier (see Fig. 12, *b*).

In experiments[21] where external EWP were supplied to thin samples at the pressure equal to p_{RE} appeared in the sample with the corresponding composition at rheological explosion, the dependences of the yields of stable dimethylbenzyl radicals coincide with those described above to experimental errors. This also confirms that the process of rheological explosion results in elastic waves appearing during relaxation of defects. Thus, it has unambiguously been shown[21] that, first, the mechanisms of redox transformations in the matrix of network polymer (glassy polyepoxide) are sensitive to the topological structure of the polymer network, and, second, these processes include stages in which light mobile species, electrons and hydrogen atoms, can be formed.

Mechanisms of chemical processes occurring under EWP action

It follows from the data presented above that the proposed convection model of mechanochemical reactions adequately explains the appearance of reactive species, electrons, protons, metal ions, and radicals, which appear during decomposition of the solid under the EWP action, and that elastic wave pulses excite vibrations of atoms (or their groups) in solids. However, these data do not clarify a relation between elastic and electromagnetic waves in the mechanically excited solid, because an unpaired electron can appear due to an electromagnetic wave only.

We answered this question in out recent work.[22] It has previously been established[11] that the edge of EWP-initiated chemical transformations in solid ammonium bichromate ($(NH_4)_2Cr_2O_7$) propagates with a velocity of 1.3 km s^{-1}, and that of EWP propagation along molded $(NH_4)_2Cr_2O_7$ is 2.2 km s^{-1}. It has been proved[11] that the $(NH_4)_2Cr_2O_7$ sample is heated to at most 300 °C rather than to 1300 °C, as in the case of thermal decomposition of $(NH_4)_2Cr_2O_7$ to chromium oxide in the reaction

$$(NH_4)_2Cr_2O_7 \longrightarrow Cr_2O_3 + N_2 + 4\ H_2O + 298\ kJ\ mol^{-1}. \qquad (21)$$

It was also found[22] that primary chemical transformations in $(NH_4)_2Cr_2O_7$ appear after some time (delay time) τ whose value ranges within (170—400)±10 μs and changes with p_{RE} as follows: $\tau^{-1} = \alpha p_{RE}^2 + \beta p_{RE} + C$ ($\alpha = -4.48 \cdot 10^{-5}$, $\beta = 1.78 \cdot 10^{-3}$, $C = -1.26 \cdot 10^{-2}$). This dependence contains square and linear terms with respect to p_{RE}, *i.e.*, the τ value is affected by both the static pressure on the sample (p_{RE}) and the energy flow of the elastic wave.

For EWP with $p_{RE} < 10$ kbar, ESR signals with $g_\perp = 1.991$ and $g_\parallel = 1.933$, which are characteristic of Cr^V, were detected. The intensity of these signals increases to $p_{RE} \approx 10$ kbar and then decreases sharply (Fig. 13). In molded $(NH_4)_2Cr_2O_7$ samples, broad ESR signals with $g_{aver} \approx 2.00$ and $\Delta H \approx 50$ mT, characteristic of ultrafine Cr_2O_3, appear at $p_{RE} \approx 10$ kbar.[33] The dependences of accumulation of Cr^V and Cr^{III} ions (see Fig. 13, curves *1* and *2*, respectively) within $p_{RE} = 10—11$ kbar are antiparallel, which indicates the reduction of Cr^V to Cr^{III}.

Thus, the EWP-induced decomposition of $(NH_4)_2Cr_2O_7$ has a threshold character with respect to power. This is favored by the fact that when the elastic energy is supplied to the $(NH_4)_2Cr_2O_7$ sample in portions (*i.e.*, as several pulses at $p_{RE} < 10$ kbar), whose total value is equal to the critical energy inlet at p_{RE} =

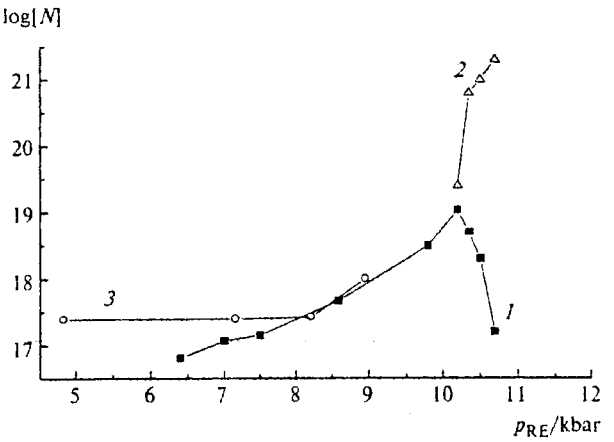

Fig. 13. Dependences of changes in concentrations of Cr^V (*1*) and ultrafine Cr_2O_3 (*2*) in the $(NH_4)_2Cr_2O_7$ sample on p_{RE} with a single EWP and the dependence of the change in the concentration of Cr^V on the action of several EWP (*3*) at different p_{RE} that introduce into the sample the same amount of elastic energy equivalent to the energy at $p_{RE} = 10$ kbar ([*N*] is the number of paramagnetic centers per g of $(NH_4)_2Cr_2O_7$).

10 kbar, no self-propagating processes appear. The Cr^V particles are accumulated as shown in Fig. 13 (curve *3*): introduction of several pulses with $p_{RE} < 10$ kbar separated in time by experimental conditions (time between pulses ≥30 s) does not result in the appearance of self-propagating chemical processes. Thus, these processes have a pronounced power character.

All aforesaid suggests[22] the following scheme of self-propagating processes that supplements and develops the convection mechanism.

Since the front of chemical reactions appears after some time delay τ, it is reasonable to assume that the introduction of EWP that are critical by power results in the appearance of defects of the crystalline lattice in the upper narrow layer of $(NH_4)_2Cr_2O_7$: vacancies, dislocations, and crystalline cavities. This process is characterized by a threshold energy and accompanied by deep amorphization of the substance.

From the viewpoint of the band theory of solids,[34] amorphization is related to "diffusion" of edges of the conduction and valence bands and to the formation of a series of sub-bands in the forbidden band that correspond to ensembles of negatively (D^-) and positively (D^+) charged defects with different dimensionalities. The scheme of this process is presented in Fig. 14, *a*. The appearance of diffuse sub-bands favors free transfer of the charge density over the amorphous polycrystalline substance. From the chemical viewpoint, this is accompanied by the excitation (activation) of $(NH_4)_2Cr_2O_7$ molecules, formation of free e_q^- and H^+, charged dipoles on individual ammonium bichromate molecules or on clusters of these molecules due to uncompensated charges, and appearance of photons during deactivation of $(NH_4)_2Cr_2O_7$ molecules. The appearance of dipole species provides a relation between mechanical and electric vibrations and overlapping (coalescence) of acoustic and optical phonon modes when the so-called soft mode appears (see Fig. 14, *b*). (This phenomenon is inherent in a wide class of inorganic substances.[35]) The latter results, perhaps, in the appearance of quasi-particles related to local oscillations of the solid lattice,[36,37] polaritons and polarons, which almost completely absorb the photon energy.[37] When the critical concentration of dipoles, e_q^-, and photons is achieved in the upper narrow layer of the $(NH_4)_2Cr_2O_7$ sample, a self-induced correlation between dipole moments takes place, which acts on the next layer of the sample to produce its chemical decomposition. All this can be compared to the well studied processes of super-radiation at optical and hypersound frequencies.[38]

Thus, the scheme of mechanochemical reactions occurring under the EWP action was supplemented[22] by the notion of a dipole that relates elastic vibrations and electromagnetic waves in solids, *i.e.*, an electromagnetic-mechanical dipole (EMD), for which the following equation is fulfilled:

$$\omega = \upsilon_{EW}/\lambda_{EW} = c/\lambda_{EM}. \qquad (22)$$

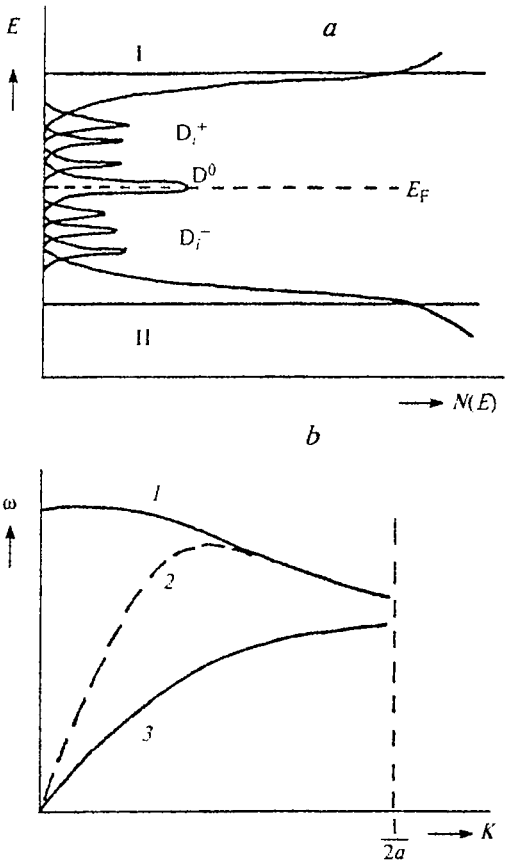

Fig. 14. *a*. Scheme of density of defect states ($N(E)$) appearing in amorphous $(NH_4)_2Cr_2O_7$ under EWP action (D_i^+, D_i^- are the series of charged defect states; D^0 are metastable molecules; I is the conduction band; II is the valence band). *b*. Typical dispersion curves for optical (*1*), soft (*2*), and acoustical (*3*) branches of the vibration spectra when their overlapping appears (ω is the frequency, *a* is the lattice parameter, and *K* is the wavenumber).

where ω is the frequency of dipole vibrations; υ_{EW} and c are the velocities of the elastic wave and light, respectively; and λ_{EW} and λ_{EM} are the lengths of elastic and electromagnetic waves emitted by a dipole, respectively. In addition, it has been shown[22] that the introduction in the scheme of mechanochemical processes of such quasiparticles as polaritons, whose energy consists partially of electromagnetic energy and partially of energy of elastic excitation of the medium (polaritons are formed due to the interaction of photons with optical phonons, excitons, and magnons), clarifies the question of where the "deficient" heat goes in mechanochemical processes, *i.e.*, the difference between mechanochemical and thermal processes.

The introduced[22] notion of an electromagnetic-mechanical dipole in combination with the previously proposed convection model completely describes chemical processes that occur under the EWP action and, probably, mechanochemical reactions in general.

In fact, if elastic waves initiating the appearance of EMD are considered as solitons (a dislocation can be considered as a one-dimensional soliton), the general scheme of the appearance of mechanochemical reaction is the following:

$$S \rightarrow EMD \longrightarrow e_q^-,\ (h\omega)_p,\ M^+,\ M^* \longrightarrow$$
$$\longrightarrow \text{stable products},$$

where S is soliton, EMD is electromagnetic-mechanical dipole, e_q^- is polaron (electron related to phonons), $(h\omega)_p$ is polariton, M^+ is ion, and M^* is excited molecule.

This scheme agrees well with the previously proposed mechanisms of phonon[40] and exciton-dislocation[41] decomposition of solids and ionic crystals, and supplementing them, it does not contradict the concepts on the relation between the edge of solid state reactions and internal mechanical strains[42] and nonlinear waves.[43]

This work was financially supported by the Russian Foundation for Basic Research (Project No. 99-03-33342a).

References

1. P. Yu. Butyagin, *Usp. Khim.*, 1994, **63**, 1031 [*Russ. Chem. Rev.*, 1994, **63** (Engl. Transl.)].
2. N. S. Enikolopov, *Usp. Khim.*, 1991, **60**, 586 [*Russ. Chem. Rev.*, 1991, **60** (Engl. Transl.)].
3. A. A. Zharov, *Usp. Khim.*, 1984, **53**, 236 [*Russ. Chem. Rev.*, 1984, **53** (Engl. Transl.)].
4. E. G. Avvakumov, *Mekhanicheskie metody aktivatsii khimicheskikh protsessov* [*Mechanical Methods of Activation of Chemical Processes*], Nauka, Novosibirsk Division, Novosibirsk, 1979, 250 pp. (in Russian).
5. G. A. Adadurov and V. I. Gol'danskii, *Usp. Khim.*, 1981, **50**, 1810 [*Russ. Chem. Rev.*, 1981, **50** (Engl. Transl.)].
6. P. Yu. Butyagin, *Khimicheskaya fizika tverdogo sostoyaniya veshchestva. Diffuziya i reaktsionnaya sposobnost'* [*Chemical Physics of Solid State. Diffusion and Reactivity*], Izd. MFTI, Moscow, 1991, **2**, 75 (in Russian).
7. P. Yu. Butyagin, *Active States in Mechanochemical Reactions, Soviet Scientific Reviews. Section B, Chemistry Reviews*, 1989, **14**, Part 1, 25.
8. S. S. Batsanov, *Usp. Khim.*, 1986, **55**, 579 [*Russ. Chem. Rev.*, 1986, **55** (Engl. Transl.)].
9. J. G. Calvert and J. N. Pitts, Jr., *Photochemistry*, J. Wiley and Sons, New York—London—Sydney, 1966.
10. A. K. Pikaev, S. A. Kabakchi, I. E. Makarov, and B. G. Ershov, *Impul'snyi radioliz i ego primenenie* [*Pulse Radiolysis and Its Application*], Atomizdat, Moscow, 1980, 278 pp. (in Russian).
11. N. S. Enikolopyan, A. I. Aleksandrov, E. E. Gasparyan, V. I. Shelobkov, and A. A. Mkhitaryan, *Dokl. Akad. Nauk SSSR*, 1991, **319**, 1384 [*Dokl. Chem.*, 1991 (Engl. Transl.)].
12. A. I. Aleksandrov, A. I. Prokof'ev, I. Yu. Metlenkova, N. N. Bubnov, D. S. Tipikin, G. D. Perekhodtsev, and Ya. S. Lebedev, *Zh. Fiz. Khim.*, 1995, **69**, 739 [*Russ. J. Phys. Chem.*, 1995, **69** (Engl. Transl.)].
13. A. I. Aleksandrov, A. I. Prokof'ev, I. Yu. Metlenkova, N. N. Bubnov, D. S. Tipikin, G. D. Perekhodtsev, S. D. Chemerisov, and Ya. S. Lebedev, *Izv. Akad. Nauk. Ser. Khim.*, 1996, 864 [*Russ. Chem. Bull.*, 1996, **45**, 819 (Engl. Transl.)].
14. A. I. Aleksandrov, V. P. Zhukov, A. I. Prokof'ev, N. N. Bubnov, G. D. Perekhodtsev, and Ya. S. Lebedev, *Izv. Akad. Nauk, Ser. Khim.*, 1996, 1192 [*Russ. Chem. Bull.*, 1996, **45**, 1132 (Engl. Transl.)].
15. A. I. Aleksandrov, T. B. Chenskaya, A. I. Prokof'ev, N. N. Bubnov, A. A. Dubinskii, E. V. Gal'tseva, I. A. Aleksandrov, and Ya. S. Lebedev, *Izv. Akad. Nauk, Ser. Khim.*, 1997, 1464 [*Russ. Chem. Bull.*, 1997, **46**, 1399 (Engl. Transl.)].
16. A. I. Aleksandrov, A. I. Prokof'ev, I. Yu. Metlenkova, N. N. Bubnov, D. S. Tipikin, S. D. Chemerisov, G. D. Perekhodtsev, and Ya. S. Lebedev, *Zh. Fiz. Khim.*, 1996, **70**, 842 [*Russ. J. Phys. Chem.*, 1996, **70** (Engl. Transl.)].
17. A. I. Aleksandrov, A. I. Prokof'ev, S. P. Solodovnikov, N. N. Bubnov, I. A. Aleksandrov, and Ya. S. Lebedev, *Izv. Akad. Nauk. Ser. Khim.*, 1996, 2780 [*Russ. Chem. Bull.*, 1996, **45**, 2639 (Engl. Transl.)].
18. A. I. Aleksandrov, A. I. Prokof'ev, N. N. Bubnov, R. R. Rakhimov, I. A. Aleksandrov, A. A. Dubinskii, and Ya. S. Lebedev, *Izv. Akad. Nauk, Ser. Khim.*, 1999, 324 [*Russ. Chem. Bull.*, 1999, **48**, 323 (Engl. Transl.)].
19. A. I. Aleksandrov, A. I. Prokof'ev, V. N. Lebedev, E. V. Balagurova, N. N. Bubnov, I. Yu. Metlenkova, S. P. Solodovnikov, and A. N. Ozerin, *Izv. Akad. Nauk, Ser. Khim.*, 1995, 2355 [*Russ. Chem. Bull.*, 1995, **44**, 2251 (Engl. Transl.)].
20. A. I. Aleksandrov, E. E. Gasparyan, V. S. Svistunov, A. A. Khazardzhyan, A. I. Prokof'ev, and N. N. Bubnov, *Dokl. Akad. Nauk SSSR*, 1990, **314**, 648 [*Dokl. Chem.*, 1990 (Engl. Transl.)].
21. A. I. Aleksandrov, I. Yu. Metlenkova, A. N. Zelenetskii, A. I. Prokof'ev, S. P. Solodovnikov, and N. N. Bubnov, *Izv. Akad. Nauk, Ser. Khim.*, 1997, 1622 [*Russ. Chem. Bull.*, 1997, **46**, 1546 (Engl. Transl.)].
22. A. I. Aleksandrov, I. A. Aleksandrov, A. I. Prokof'ev, and N. N. Bubnov, *Izv. Akad. Nauk, Ser. Khim.*, 1998, 1140 [*Russ. Chem. Bull.*, 1998, **47**, 1108 (Engl. Transl.)].
23. M. I. Kabachnik, N. N. Bubnov, S. P. Solodovnikov, and A. I. Prokof'ev, *Tautometriya svobodnykh radikalov* [*Tautomerism of Free Radicals*], in *Itogi Nauki, Tekh., Ser. Khim.* [*Results of Science and Technique, Chemistry Division*], VINITI, Moscow, 1984, **5**, 3 (in Russian).
24. A. I. Aleksandrov, N. N. Bubnov, G. G. Lazarev, Ya. S. Lebedev, A. I. Prokof'ev, and M. V. Serdobov, *Izv. Akad. Nauk SSSR, Ser. Khim.*, 1976, 515 [*Bull. Acad. Sci. USSR, Div. Chem. Sci.*, 1976, **25** (Engl. Transl.)].
25. V. S. Boiko, R. I. Garber, and A. M. Kosevich, *Obratimaya plastichnost' kristallov* [*Inverse Plasticity of Crystals*], Nauka, Moscow, 1991, 279 pp. (in Russian).
26. G. G. Lazarev, Ya. S. Lebedev, A. I. Prokof'ev, and R. R. Rakhimov, *Khim. Fiz.*, 1984, 867 [*Sov. Chem. Phys.*, 1984, No. 3 (Engl. Transl.)].
27. O. G. Poluektov, J. Schmidt, D. S. Tipikin, and Ya. S. Lebedev, *Chem. Phys. Lett.*, 1993, **215**, 199.
28. S. D. Chemerisov, O. Ya. Grinberg, D. S. Tipikin, Ya. S. Lebedev, H. Kurrek, and K. Mobius, *Chem. Phys. Lett.*, 1994, **218**, 353.
29. K. Sarbasov, B. L. Tumanskii, S. P. Solodovnikov, N. N. Bubnov, and A. I. Prokof'ev, *Izv. Akad. Nauk SSSR, Ser. Khim.*, 1983, 2236 [*Bull. Acad. Sci. USSR, Div. Chem. Sci.*, 1983, **32**, 2018 (Engl. Transl.)].
30. S. P. Solodovnikov, A. Y. Vasilkov, A. Y. Olenin, and V. A. Sergeev, *J. Magn. Magn. Mater.*, 1994, **129**, 317.

31. S. P. Solodovnikov, L. M. Bronshtein, P. M. Valetskii, Yu. A. Kabachii, and S. V. Vinogradova, *Metalloorg. Khim.*, 1990, **3**, 609 [*Organomet. Chem. USSR*, 1990, **3** (Engl. Transl.)].
32. A. I. Aleksandrov, A. I. Prokof'ev, and N. N. Bubnov, *Usp. Khim.*, 1996, **65**, 519 [*Russ. Chem. Rev.*, 1996, **65** (Engl. Transl.)].
33. L. A. Blyumenfel'd, V. V. Voevodskii, and A. G. Semenov, *Primenenie elektronnogo paramagnitnogo rezonansa v khimii* [*The Application of Electron Paramagnetic Resonance in Chemistry*], Izd. Sib. Otd. AN SSSR, Novosibirsk, 1962, 240 pp. (in Russian).
34. A. Feltz, *Amorphe und Glasartige Anorganische Festkorper*, Akademie-Verlag, Berlin, 1983.
35. J. C. Burfoot and G. W. Taylor, *Polar Dielectrics and Their Applications*, Macmillan Press LTD, New Jersey, 1979, 515 pp.
36. D. D. Appel' and Yu. A. Firsov, *Polyarony* [*Polarons*], Mir, Moscow, 1975 (in Russian).
37. S. I. Pekar, *Kristallooptika i dobavochnye svetovye volny* [*Crystal Optics and Additional Light Waves*], Naukova Dumka, Kiev, 1982, 340 pp. (in Russian).
38. A. V. Andreev, *Usp. Fiz. Nauk*, 1990, **160**, No. 12, 1 [*Russ. Phys. Sci.*, 1990, No. 12, 1 (Engl. Transl.)].
39. V. M. Agshranovich and V. L. Ginzburg, *Kristallooptika s uchetom prostranstvennoi dispersii i teorii eksitonov* [*Crystal Optics with Spatial Dispersity and Exciton Theory*], Nauka, Moscow, 1979, 380 pp. (in Russian).
40. G. M. Batrenev and I. V. Razumovskii, *Fiziko-khimicheskaya mekhanika materialov* [*Physicochemical Properties of Materials*], 1969, **5**, 60 (in Russian).
41. I. M. Molotskii, *Kinet. Katal.*, 1981, **22**, 1153 [*Kinet. Catal.*, 1981, **22** (Engl. Transl.)].
42. A. G. Knyazev, *Fizika Goreniya i Vzryva*, 1994, 44 [*Phys. Combust. Explos.*, 1994 (Engl. Transl.)].
43. L. I. Manevich and V. V. Smirnov, *Vysokomol. Soedin., A*, 1994, **36**, 552 [*Polym. Sci. USSR, Ser. A*, 1994, **36** (Engl. Transl.)].

Received March 10, 1999;
in revised form April 19, 1999